and output impedances. The a and b coefficients are chosen to achieve the maximum gain-bandwidth which sets $a = 0.75$ and $b = 0.32$.

At this point, the choice of device g_m must be made. It must be chosen with some care as it determines the number of devices N, which also affects the parasitic resistances R_g and R_{ds}. Using (3), we choose to set $N = 8$ and solve for $g_m = 38$ mmhos. From Fig. 2, at $(a, b) = (0.75, 0.32)$, $X \approx 0.74$. Since we require $f_{-3\,\mathrm{dB}} = 20$ GHz, this sets $f_c = 27$ GHz. Based upon these values, the remaining values are

$$C_{gs} = 0.23 \text{ pF}$$
$$R_g = 4.7\ \Omega$$
$$C_{ds} = 0.235 \text{ pF}$$
$$R_{ds} = 312\ \Omega.$$

The transistor is now completely specified. The fact that C_{gs} and C_{ds} are equal results because the input and output line impedances have been set equal to one another.

III. Conclusion

We have shown that the maximum normalized gain-bandwidth curve in [1] is a small portion of the more general gain-bandwidth contours. There is a maximum which corresponds to the optimum design of a distributed amplifier. Constraint-free design equations for transistors specifically intended for use in distributed amplifiers were also presented.

References

[1] J. B. Beyer, S. N. Prasad, R. C. Becker, J. E. Nordman, and G. K. Hohenwarter, "MESFET-distributed amplifier design guidelines," *IEEE Trans. Microwaves Theory Tech.*, MTT-32, pp. 268–275, Mar. 1984.

[2] R. C. Becker, "Constraints in the design of GaAs MESFET MMIC-distributed amplifiers," Ph.D. thesis, Univ. of Wisconsin, pp. 128–144, 1985.

Dispersion of Picosecond Pulses in Coplanar Transmission Lines

G. HASNAIN, A. DIENES, AND J.R. WHINNERY

***Abstract*—The dispersion of coplanar-type transmission lines has been extended to the terahertz regime to examine the distortion of picosecond electrical pulses. Dispersion of coplanar waveguides is compared to equivalent microstrip lines. Agreement with available experimental data is demonstrated for coplanar strips. An approximate dispersion formula for coplanar waveguides is also reported for CAD applications.**

I. Introduction

Picosecond electrical pulses generated by opto-electronic switches [1] have several hundred gigahertz bandwidth and are therefore much dispersed within a few millimeters of travel, even on high-frequency transmission lines such as microstrips and coplanar waveguides. Dispersion characteristics have been investigated thoroughly for the popular microstrip line [2], but published data for coplanar lines are usually limited to about 50 GHz. In previous papers [3], [4], we examined the dispersion of picosecond pulses in microstrip lines. In this paper, we extend the dispersion relation of coplanar-type transmission lines into the terahertz regime and use the result to compute distortion of picosecond pulses propagating in such lines.

Manuscript received September 20, 1985; revised January 2, 1986. This work was supported in part by the National Science Foundation Program under Grant ECS-8114526.

G. Hasnain and J. R. Whinnery are with the Department of Electrical Engineering and Computer Sciences, Electronics Research Laboratory, University of California, Berkeley, CA 94720.

A. Dienes is with the Department of Electronics and Computer Engineering, University of California, Davis, CA 95616.

IEEE Log Number 8607980.

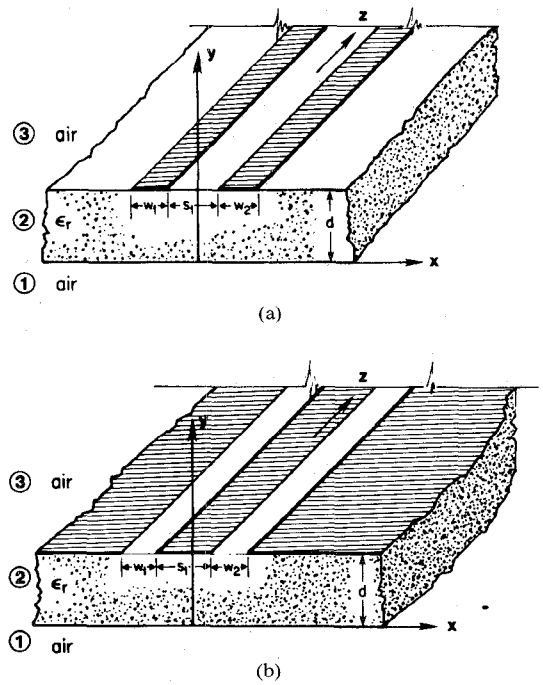

Fig. 1. Two examples of a coplanar-type transmission lines. (a) Coplanar strips (CPS). (b) Coplanar waveguide (CPW).

II. Theory

The spectral domain analysis method used here was first proposed for slot lines by Itoh and Mittra [5] and later extended by Knorr and Kuchler [6] to coupled slots and coplanar strips. For the purpose of clarity, the main steps of the analysis are briefly reiterated. Typical coplanar transmission lines consist of two or more metal strips separated by slots on a dielectric substrate (Fig. 1). The problem is to find the solution to the wave equation in an inhomogeneous medium with inhomogeneous boundary conditions. Since the metal discontinuities lead to difficulties in defining the boundary conditions in the transverse direction, the scalar potentials $\varphi^{e,h}(x, y)$ are transformed into the Fourier domain. Thus, the Helmholtz wave equation is converted to an ordinary differential equation whose solutions are given by:

$$\varphi_1(\alpha, y) = A(\alpha)\, e^{-\gamma_1 (y-d)} \tag{1}$$

$$\varphi_2(\alpha, y) = B(\alpha)\sinh(\gamma_2 y) + C(\alpha)\cosh(\gamma_2 y) \tag{2}$$

$$\varphi_3(\alpha, y) = D(\alpha)\, e^{\gamma_1 y} \tag{3}$$

where $\gamma_i^2 = \alpha^2 + \beta^2 - \omega^2 \mu_0 \epsilon_0 \epsilon_i$, $i = 1,2,3$ define the regions, α is the transform variable corresponding to the x-variation, and β is the propagation constant in the longitudinal direction. Using the continuity conditions at $y = 0$

$$E_{z2} = E_{z3}; \quad E_{x2} = E_{x3}; \quad H_{z2} = H_{z3}; \quad H_{x2} = H_{x3} \tag{4}$$

and the interface conditions at $y = d$

$$E_{z2} = E_{z1} = E_z(\alpha); \quad E_{x2} = E_{x1} = E_x(\alpha) \tag{5}$$
$$H_{z2} - H_{z1} = J_x(\alpha); \quad H_{x2} - H_{x1} = J_z(\alpha)$$

we eliminate the eight constants to obtain a set of coupled equations

$$G_{11}(\alpha,\beta)E_x(\alpha) + G_{12}(\alpha,\beta)E_z(\alpha) = J_x(\alpha) \tag{6}$$
$$G_{21}(\alpha,\beta)E_x(\alpha) + G_{22}(\alpha,\beta)E_z(\alpha) = J_z(\alpha) \tag{7}$$

where $G_{ij}(\alpha,\beta)$ are the elements of the dyadic Green function in the Fourier transform domain.

Expanding the electric-field components in an infinite series using a complete set of basis functions

$$E_x(\alpha) = \sum_{n=1}^{\infty} a_n \eta_n(\alpha) \quad \text{and} \quad E_z(\alpha) = \sum_{n=1}^{\infty} b_n \zeta_n(\alpha) \tag{8}$$

and applying Galerkin's method [7], we have

$$\sum_{n=1}^{\infty} P_{mn}(\beta)a_n + \sum_{n=1}^{\infty} Q_{mn}(\beta)b_n = 0 \tag{9}$$

$$\sum_{n=1}^{\infty} R_{mn}(\beta)a_n + \sum_{n=1}^{\infty} S_{mn}(\beta)b_n = 0 \tag{10}$$

for $m = 1,2,3 \cdots \infty$, where

$$P_{mn}(\beta) = \int_{-\infty}^{\infty} G_{11}(\alpha,\beta)\eta_m^*(\alpha)\eta_n(\alpha)\,d\alpha \tag{11}$$

$$Q_{mn}(\beta) = \int_{-\infty}^{\infty} G_{12}(\alpha,\beta)\eta_m^*(\alpha)\zeta_n(\alpha)\,d\alpha \tag{12}$$

$$R_{mn}(\beta) = \int_{-\infty}^{\infty} G_{21}(\alpha,\beta)\zeta_m^*(\alpha)\eta_n(\alpha)\,d\alpha \tag{13}$$

$$S_{mn}(\beta) = \int_{-\infty}^{\infty} G_{22}(\alpha,\beta)\zeta_m^*(\alpha)\zeta_n(\alpha)\,d\alpha. \tag{14}$$

For nontrivial solutions of the electric fields, the determinant of the coefficient matrix of (9) and (10) must vanish. The values of β, obtained from the determinantal equation for a given frequency, define the desired dispersion relation.

The theory developed is exact but a practical solution cannot be obtained from an infinite determinant. In practice, a priori knowledge of the actual field distribution is used to approximate the field expansion by only a few terms. However, the actual numerical evaluation of the determinant becomes very complicated beyond a certain frequency due to the appearance of transversely propagating modes that are manifested in the spectral domain as poles of the Green function (Fig. 2(a)). Fortunately, the poles are simple and their effect on the accuracy of the integration can be greatly reduced by integrating over subintervals chosen symmetrically about the poles. The poles must first be determined by numerically solving for the roots of the Green function denominator. This becomes more difficult with increasing frequency as the number of roots grows and their separation rapidly decreases (Fig. 2(b)). In a realistic guide, the transverse direction is usually bounded by conducting walls. This causes standing waves and consequently the scalar potentials are then expanded in a Fourier series. The poles of the Green function do not, in general, coincide with the spectral harmonics, but the sharp resonances still make the summations difficult to evaluate. Also, while substrate and conductor losses limit the amplitude of the resonances somewhat, this does not alleviate the difficulties in the evaluation of the integrals. Nevertheless, by careful choice of numerical algorithms, it has been possible to extract solutions up to several terahertz frequencies for typical configurations. A good

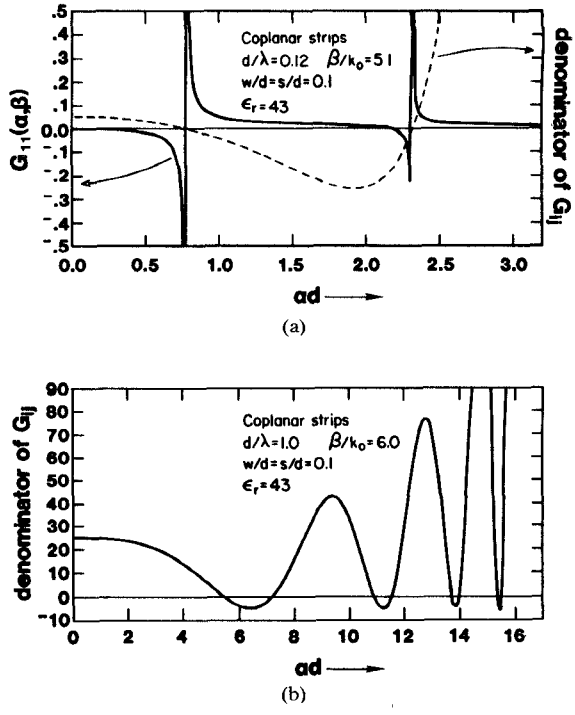

Fig. 2. (a) Green function component $G_{11}(\alpha,\beta)$ and its denominator (dashed curve) versus αd for $d/\lambda = 0.12$ (72 GHz for $d = 500$ μm) and $\beta/k_o = 5.1$. Configuration: Coplanar strips with $w/d = 0.1$, $s/d = 0.1$, and $\epsilon_r = 43$. (b) Denominator of $G_{11}(\alpha,\beta)$ versus αd for $d/\lambda = 1.0$ (600 GHz for $d = 500$ μm) and $\beta/k_o = 6.0$. Same configuration as Fig. 2(a).

choice for the basis functions in the spectral domain are the Bessel functions. With these functions, fairly accurate solutions can be obtained from a 2×2 matrix—that is, using a one term expansion. However, we have used up to four terms which required the evaluation of 64 integrals (each of which may have as many as 10 poles) for a given value of frequency. The numerical calculations involve considerable computing time even for the one term expansion.

Finally, pulse distortion due to dispersion is computed from [4]

$$V(f,z) = V(f,0)e^{-j\beta(f)z} \tag{15}$$

where

$$\beta = 2\pi\frac{f}{c}\sqrt{\epsilon_{\text{eff}}(f)} \tag{16}$$

and $V(f,z)$ is the Fourier transform of the pulse $v(t,z)$ at a distance z.

III. Results

Owing to the significant computing effort needed to obtain the value of β at any given frequency, it was found expedient to use the empirical formula (also used for microstrip dispersion [8])

$$\sqrt{\epsilon_{\text{eff}}(f)} = \sqrt{\epsilon_q} + \frac{\left(\sqrt{\epsilon_r} - \sqrt{\epsilon_q}\right)}{(1 + aF^{-b})} \tag{17}$$

curve fitted to the dispersion data. $F = f/f_{\text{TE}}$ is the normalized frequency, $f_{\text{TE}} = 4\sqrt{\epsilon_r - 1}/d$ is the cut-off frequency for the lowest order TE mode, ϵ_q is the effective permittivity at the quasi-static limit [2], and a, b are constants which depend on the configuration and dimensions. This empirical formula appears to fit quite well the dispersion relations for both coplanar waveguide (CPW) and coplanar strip (CPS).

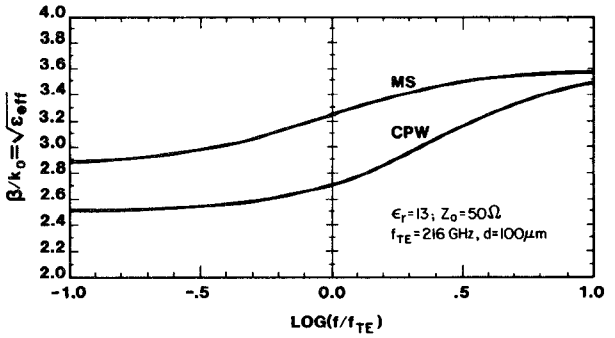

Fig. 3. Propagation constant β/k_o versus normalized frequency (f/f_{TE}) for a coplanar waveguide and a microstrip on a gallium arsenide substrate both having 50-Ω characteristic impedance (see text for dimensions).

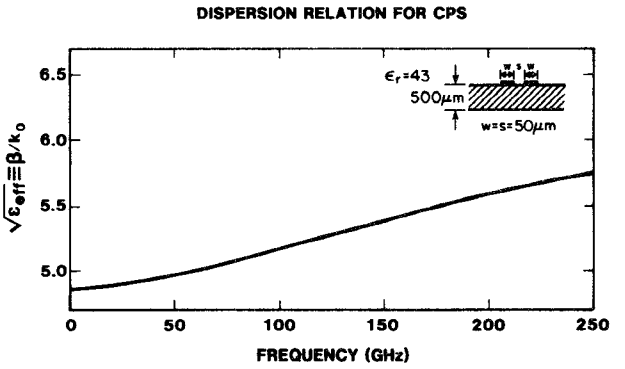

Fig. 5. Propagation constant β/k_o versus frequency for coplanar strips with $w=s=50\ \mu$, $d=500\ \mu$, and $\epsilon_r=43$.

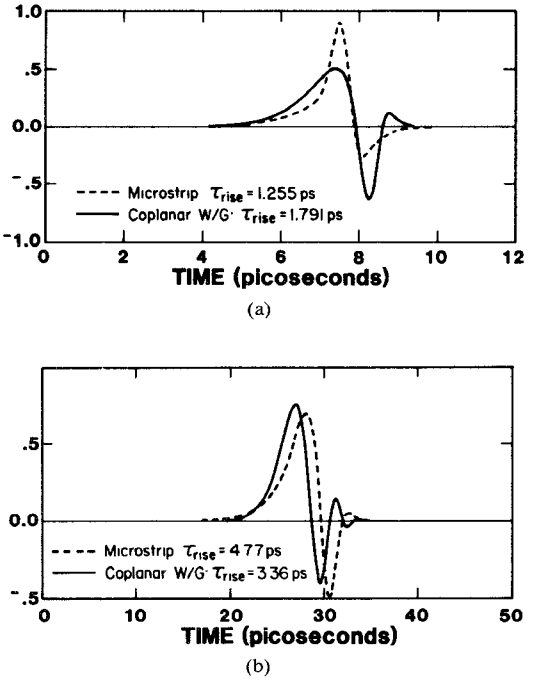

Fig. 4. Distorted shape of a Gaussian pulse after propagating equal distance on the coplanar waveguide and microstrip line described in Fig. 3. (a) Initial pulse full-width, half maximum FWHM = 0.5 ps; travel distance: 0.5 mm. (b) Initial pulse FWHM = 2.0 ps; travel distance: 2.0 mm.

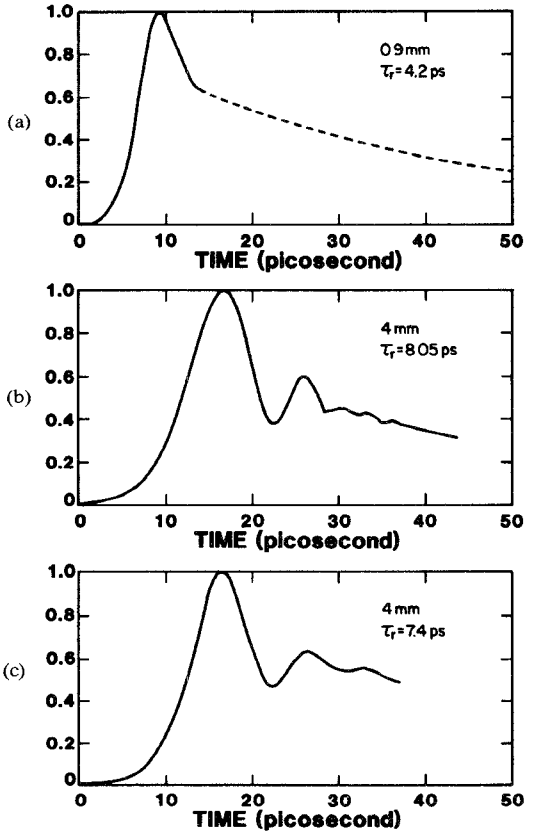

Fig. 6. (a) Experimentally measured pulse shape at 0.9 mm with falling edge extrapolated (dashed line) for computational purpose (Courtesy: K. Meyer, University of Rochester, NY; see [9] for experimental setup). (b) Theoretically computed pulse shape at 4 mm using dispersion relation shown in Fig. 3. (c) Experimentally measured pulse shape at 4 mm (Courtesy: K. Meyer, University of Rochester, NY).

The constants a and b in the empirical formula for dispersion was also computed for coplanar waveguides of varying dimensions. We observed that $b \approx 1.8$ independent of the dimensions, while a is computed from

$$\log(a) \approx u \log(s/w) + v \tag{18}$$

where u and v depend on the substrate thickness d as follows:

$$u \approx 0.54 - 0.64q + 0.015q^2 \tag{19}$$

$$v \approx 0.43 - 0.86q + 0.540q^2 \tag{20}$$

where $q = \log(s/d)$.

We have thus obtained an approximate formula for desk calculation of dispersion, which should prove useful in the computer-aided-design (CAD) of microwave-integrated circuits involving coplanar waveguides. The formula has been verified to be accurate to within 5 percent for the following range of parameters

$$0.1 < s/w < 5; \quad 0.1 < s/d < 5;$$
$$1.5 < \epsilon_r < 50; \quad 0 < f/f_{TE} < 10.$$

Outside the above range the formula may still be valid, but its validity has not been tested due to computational limitations.

Gallium arsenide is one of the semiconductors often used for optoelectronic switches. We therefore analyzed the dispersion of the typical 50-ohm coplanar waveguide (50-μ slot, 85-μ strip) on a 100-μ thick GaAs substrate having $\epsilon_r = 13$. The dispersion relation is shown in Fig. 3 in comparison with that of a 50-Ω microstrip (73-μ strip) on the same substrate [3]. We observe that the quasi-state value of the effective permittivity ϵ_q is lower for the coplanar line compared to the microstrip. This is to be expected since the coplanar line has greater fringe fields. At infinite frequencies the effective permittivity ϵ_{eff} approaches ϵ_r in

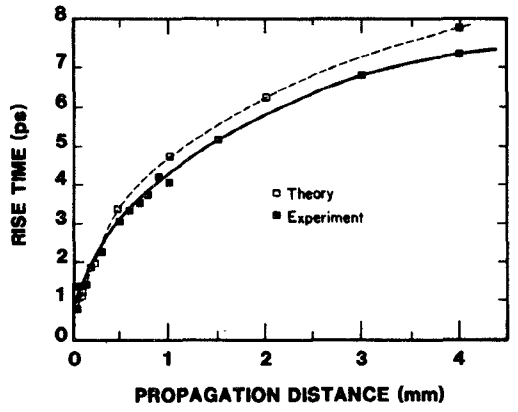

Fig. 7. Rise time of distorted pulse as a function of propagation distance. Theoretical values are compared against those experimentally measured (Courtesy: K. Meyer, University of Rochester, NY).

both cases. This implies that ultrashort pulses (having bandwidths greater than 700 GHz for this case) will suffer greater dispersion in the coplanar line. On the other hand, since the increase of ϵ_{eff} with frequency begins more gradually for coplanar lines, longer pulses with narrow bandwidth experience less variation of ϵ_{eff} and hence less distortion. This difference of behavior is illustrated in Fig. 4. The dispersion of both coplanar and microstrip lines can be reduced by reducing the substrate thickness. For coplanar lines, dispersion can also be slightly reduced by decreasing the strip and slot dimensions, but the ϵ_{eff} at low frequency remains lower then the corresponding microstrip and thus it is intrinsically more dispersive for short pulses.

The only experimental measurement of dispersion in coplanar transmission lines, to our knowledge, has been made at the University of Rochester [9], [10] on lithium tantalate substrates using an electrooptic sampling technique. Consequently, calculations were made for their experimental configuration which utilizes two coplanar strips each 50 μ wide and separated by 50 μ on a 500-μ thick $LiTaO_3$ substrate having $\epsilon_r = 43$. The numerically derived dispersion curve is shown in Fig. 5. For this case, the constants in curve-fitting (17) are $\epsilon_q = 23.68$, $a = 51.3$, $b = 1.69$, and $f_{\text{TE}} = 23.15$ GHz. Using their experimentally measured pulse shape at 0.9 mm (Fig. 6(a)) with the falling edge extrapolated (the data supplied was truncated), the pulse shape at 4 mm was computed (Fig 6(b)) from the dispersion relation. The agreement with the experimental result (Fig. 6(c)) is found to be reasonable. The frequency dependence of the characteristic impedence and that of the losses in the conductor and substrate is expected to have very little effect on the pulse distortion in coplanar lines, extrapolating from the calculations made for the microstrip line in our previous paper [3]. Pulse dispersion was also calculated for different distances of propagation and 10–90 percent risetime plotted as a function of distance. Again good agreement with experimental data supplied is obtained (Fig. 7).

IV. Conclusions

A computer program has been developed to generate dispersion relations for coplanar-type transmission lines up to terahertz frequencies for a wide range of configurations and dimensions. The number of terms in the field expansions and the order of the gaussian quadrature integration are specified in order to optimize computing time. A simple approximate formula also has been presented which can give dispersion relations for coplanar waveguides for a wide range of parameters. The results have been used to predict distortion of picosecond electrical pulses propagating in such lines. Good agreement has been obtained with available experimental results on $LiTaO_3$ substrates.

Dispersion of coplanar waveguides has been compared to an equivalent microstrip (same substrate thickness and characteristic impedance) and is found to be more for subpicosecond pulses but less for longer pulses. Finally, we note that dispersion in coplanar lines can be greatly reduced by using a superstrate of the same material, which would remove the inhomogeneity of the medium.

Acknowledgment

The authors wish to thank K. Meyer and Prof. G. Mourou for sharing their experimental results, and Profs. T. Itoh and C. Schwartz for helpful discussions.

References

[1] C. H. Lee, *Picosecond Optoelectronic Devices*.. New York: Academic Press, 1984.
[2] K. C. Gupta, R. Garg, and I. J. Bahl, *Microstrip Lines and Slotlines*. New York: Artech House, 1979.
[3] G. Hasnain, G. Arjavalingam, A. Dienes, and J. R. Whinnery, "Dispersion of picosecond pulses on microstrip transmission lines," *SPIE Proc.* vol. 439, pp. 159–163, Aug. 1983.
[4] K. K. Li, G. Arjavalingam, A. Dienes, and J. R. Whinnery, "Propagation of picosecond pulses on microwave striplines," *IEEE Trans. Microwave Theory Tech.*, vol. MTT-30, pp. 1270–1273, 1982.
[5] T. Itoh, and R. Mittra, "Dispersion characteristics of slot lines," *Electron Lett.*, vol. 7, pp. 364–365, July 1971.
[6] J. B. Knorr and K. D. Kuchler, "Analysis of coupled slots and coplanar strips on dielectric substrate," *IEEE Trans. Microwave Theory Tech.*, vol. MTT-23, pp. 541–548, July 1975.
[7] D. S. Jones, *The Theory of Electromagnetism*. New York: Pergamon, 1964.
[8] E. Yamashita, K. Atsuki, and T. Ueda, "An approximate dispersion formula of microstrip lines for computer aided design of microwave-integrated circuits," *IEEE Trans. Microwave Theory Tech.*, vol. MTT-27, pp. 1036–1038, 1979.
[9] G. Mourou and K. E. Meyer, "Subpicosecond electrooptic sampling using coplanar strip transmission lines," *Appl. Phys. Lett.* vol. 45, no. 5, pp. 492–494, Sept. 1984.
[10] K. E. Meyer and G. Mourou, private communication.

Birefringence Analysis of Anisotropic Optical Fibers Using Variational Reaction Theory

RUEY-BEEI WU AND CHUN HSIUNG CHEN

Abstract—**The variational reaction theory is applied to achieve a variational equation for the study of the single-mode optical fibers with anisotropic core media. Emphasized in this paper are the numerical results for the birefringence of the two principal modes in discussing the effects due to differences in refractive indices, anisotropy parameters, and index profiles.**

I. Introduction

Optical fibers have found applications in various areas due to the properties of low loss, high performance, electromagnetic immunity, and small size. Recently, single-mode optical fibers have received great attention because of small dispersion, but the fundamental HE_{11} modes in two orthogonal polarizations are

Manuscript received September 23, 1985; revised January 8, 1986. This work was supported in part by the National Science Council, Republic of China, under Grant NSC 74-0608-E002-02.

The authors are with the Department of Electrical Engineering, National Taiwan University, Taipei, Taiwan, Republic of China.

IEEE Log Number 8607981.